Centrality, pseudorapidity, and transverse momentum dependence of the global polarization of Ξ hyperons in Beam Energy Scan Au+Au collisions by STAR experiment

Egor Alpatov[a] *(for the STAR collaboration)*[1]

[a] National Research Nuclear University MEPhI,Kashirskoe highway 31, Moscow, 115409, Russia

In non-central heavy-ion collisions emitted particles' spin can be polarized along the initial global angular momentum due to spin-orbit coupling. Global polarization of hyperons is measured utilizing parity violating weak decay of hyperons and is used to probe the vortical properties of the system. The STAR experiment at RHIC measured the global polarization of Λ hyperons in Au+Au collisions at $\sqrt{s_{NN}}$ = 3-200 GeV, and similar measurements were conducted at the LHC for Pb+Pb collisions at $\sqrt{s_{NN}}$ = 2.76 and 5.02 TeV. Measurement of multistrange hyperons have been only limited to top RHIC energy.

In these proceedings, we will report results of Ξ global polarization for Au+Au collisions at $\sqrt{s_{NN}}$ = 14.6, 19.6 and 27 GeV by STAR. The global polarization of Ξ hyperons exhibits a trend comparable to that of Λ and is consistent with predictions from transport model calculations. This observation reinforces the idea of global nature of hyperon polarization in heavy-ion collisions.

PACS:25.75.Gz

[1]E-mail: egroker1@gmail.com

Introduction

Ultrarelativistic heavy-ion collisions offer conditions suitable for producing and studying quark-gluon plasma (QGP) – a high-temperature, high-density state of matter where quarks and gluons are deconfined. Experimental observations from RHIC and LHC indicate that the expansion dynamics of QGP are well-represented by relativistic hydrodynamic models [1].

In non-central collisions, the system acquires vorticity, which can be experimentally probed by measuring particle spin polarization along the vorticity direction. This effect, known as global polarization, can be determined through analyses of weak hyperon decays, where the daughter particle's emission tends to align with the spin of the decaying hyperon [2, 3].

For hyperon decays, the angular distribution of daughter baryons in the rest frame of the parent hyperon is described by:

$$\frac{dN}{d\cos\theta^*} \propto 1 + \alpha_H P_H \cos\theta^*, \tag{1}$$

where α_H is the hyperon decay parameter, P_H is the hyperon polarization, and θ^* represents the angle between the polarization vector and the momentum of the daughter baryon in the hyperon rest frame [4].

The initial angular momentum vector is oriented perpendicular to the reaction plane, which is defined by the beam direction and the impact parameter vector (distance from the center of one nucleus to the line of motion of another nucleus). Global polarization can be quantified by measuring the projection of the daughter baryon momentum onto this initial angular momentum direction. Assuming the first-order event plane coincides with the reaction plane, the following relation applies, accounting for event plane resolution:

$$P_H = \frac{8}{\pi\alpha_H} \frac{\left\langle \sin\left(\Psi_1^{obs} - \phi^*_{daughter}\right)\right\rangle}{Res(\Psi_1)}, \tag{2}$$

where $\phi^*_{daughter}$ is the azimuthal angle of the daughter baryon in the hyperon rest frame, and $Res(\Psi_1)$ is the event plane resolution. Known values for the decay parameters are $\alpha_\Lambda = 0.732 \pm 0.014$, $\alpha_{\bar{\Lambda}} = -0.758 \pm 0.010$, and $\alpha_{\Xi^-} = -\alpha_{\bar{\Xi}^+} = -0.401 \pm 0.010$ [5].

The STAR experiment has measured Λ hyperon global polarization in Au+Au collisions at $\sqrt{s_{NN}} = 3 - 200$ GeV [6–8]. While transport and hydrodynamic models align with the observed results, measurements of multi-strange hyperons can provide additional constraints on global polarization appearance mechanisms. Polarization measurements for Ξ and Ω hyperons have been reported at $\sqrt{s_{NN}} = 200$ GeV [9].

The Ξ hyperons are reconstructed through their cascade decay $\Xi^- \to \pi^- + \Lambda \to p + \pi^-$. This sequential decay permits two methods of polarization measurement. The first approach uses Equation 2 to measure the angle of the daughter Λ produced in Ξ decay. Alternatively, a fraction of Ξ polarization is transferred to the daughter Λ, with a transfer factor of $C_{\Xi^-\Lambda} = 0.932$, enabling Ξ global polarization determination through measurement of the daughter Λ polarization [10–12].

In these proceedings we report on the measurements of the global polarization of $\Xi^- + \bar{\Xi}^+$ hyperons in Au+Au collisions at $\sqrt{s_{NN}}$ = 14.6, 19.6 and 27 GeV by the STAR experiment, in comparison with the $\Lambda + \bar{\Lambda}$ polarization data.

Data analysis

This analysis utilizes data from Au+Au collisions at $\sqrt{s_{NN}}$ = 14.6, 19.6, and 27 GeV, collected by the STAR experiment as part of the Beam-Energy Scan II (BES-II) program. STAR's cylindrical detector [13] allows for full azimuthal coverage, and only events that met the minimum-bias trigger requirement, with a collision vertex positioned within 70 cm along the beam axis from the center of the Time Projection Chamber (TPC) and within 2 cm transversely from the beamline, were selected for analysis.

Compared to the BES-I phase, BES-II includes significant detector upgrades [7]. For the $\sqrt{s_{NN}}$ = 14.6, 19.6, and 27 GeV datasets, the Event-Plane Detector (EPD) [14] replaces the BBC [15], which was used for previous measurements, and improves event-plane resolution due to its increased granularity and acceptance. At $\sqrt{s_{NN}}$ = 14.6 and 19.6 GeV, the TPC has been upgraded (iTPC) to extend the tracking system acceptance [?].

Centrality, which reflects the degree of overlap between colliding nuclei, was determined by the charged-particle multiplicity measured in the midrapidity region. The centrality and trigger efficiency were extracted using a Monte Carlo Glauber model fit to the data.

Charged particle tracking within the pseudorapidity ranges $|\eta| < 1$ (for 27 GeV) and $|\eta| < 1.5$ (for 19.6 and 14.6 GeV) was performed with the TPC, which provides full azimuthal coverage [16]. For hyperon reconstruction, pion and proton tracks with momenta exceeding 0.15 GeV/c were identified using both the energy loss in the TPC, dE/dx, and their squared mass measured with the Time-of-Flight detector (TOF) [17].

Reconstruction of Λ hyperons was performed through the decay topology $\Lambda \to p + \pi^-$ ($\bar{\Lambda} \to \bar{p} + \pi^+$). Subsequently, Ξ hyperons were reconstructed via the cascade decay sequence $\Xi^- \to \Lambda + \pi$ ($\bar{\Xi}^+ \to \bar{\Lambda} + \pi^+$). The KFParticle package [18] was employed for the reconstruction of hyperons.

Event-plane reconstruction used the EPD within the pseudorapidity range $2.1 < \eta < 5.1$. The first-order event plane, inferred from spectator particle distributions, served as a proxy for the reaction plane. To account for finite event-plane resolution in the global polarization calculations, the resolution was determined using a two-subevent method, which relies on measurements from the East (forward rapidity) and West (backward rapidity) sides of the detector.

Global polarization values were then calculated using Equation 2, incorporating the detector event-plane resolution. The effect of track reconstruction efficiency correction on polarization was found to be negligible and therefore omitted from the analysis. However, an acceptance correction, as proposed in previous Λ polarization measurements [7], was applied. The limited detector acceptance introduces a minor dependence in Equation 2 on the momentum of the daughter particle in the hyperon rest frame, leading to the following expression:

$$\frac{8}{\pi\alpha_H}\langle\sin(\phi_b^* - \Psi_{RP})\rangle = \frac{4}{\pi}\overline{\sin\theta_b^*}P_H(p_t^H, \eta^H) = A_0(p_t^H, \eta^H)P_H(p_t^H, \eta^H), \quad (3)$$

where θ_b^* is polar angle of daughter baryon in parent's rest frame and $A_0(p_t^H, \eta^H) = \frac{4}{\pi}\overline{\sin\theta_b^*}$ is correction factor depending on p_t^H, η^H and collision centrality.

Results

Figures 1-3 present the global polarization of $\Xi^- + \bar{\Xi}^+$ hyperons, measured both directly and through the daughter hyperon's global polarization, as functions of collision centrality, transverse momentum (p_T), and pseudorapidity (η) for $\sqrt{s_{NN}} = 14.6, 19.6$ and 27 GeV respectively. Consistency is observed between the direct measurements and those obtained via the daughter hyperon's polarization. The results show an increase in global polarization with centrality, consistent with theoretical expectations and previous measurements of Λ hyperon polarization. No significant dependence on p_T or η is observed within uncertainties.

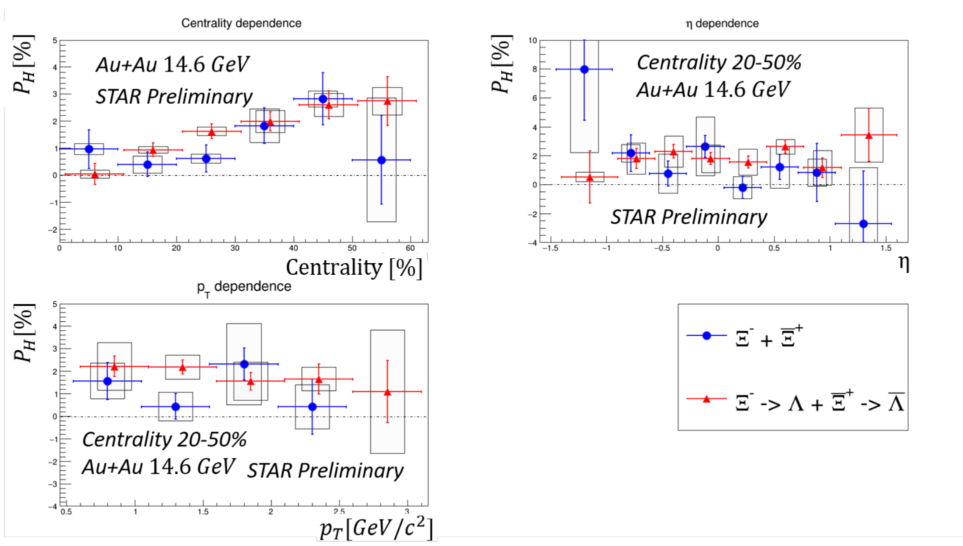

Fig. 1. Global polarization of Ξ hyperons in $\sqrt{s_{NN}} = 14.6$ GeV Au+Au collisions.

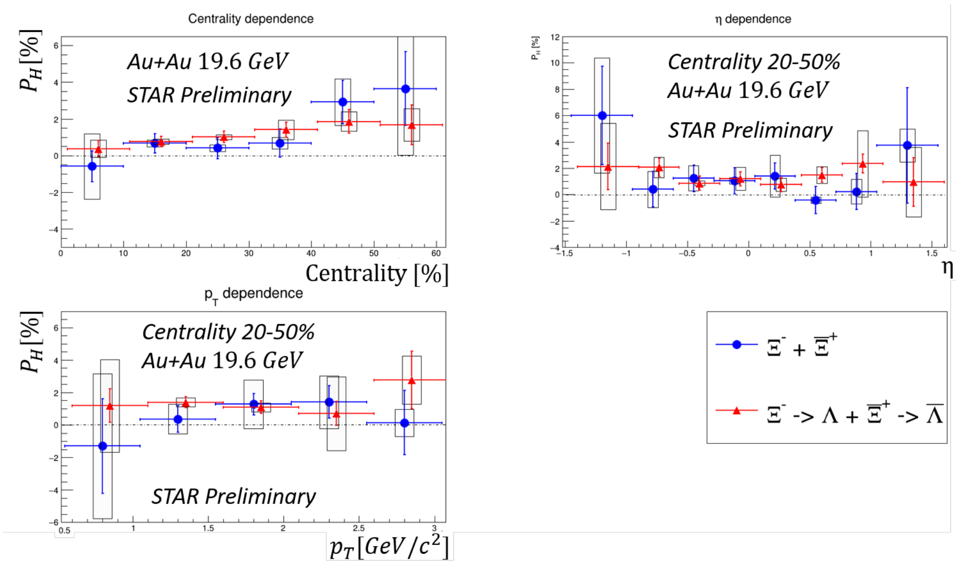

Fig. 2. Global polarization of Ξ hyperons in $\sqrt{s_{NN}} = 19.6$ GeV Au+Au collisions.

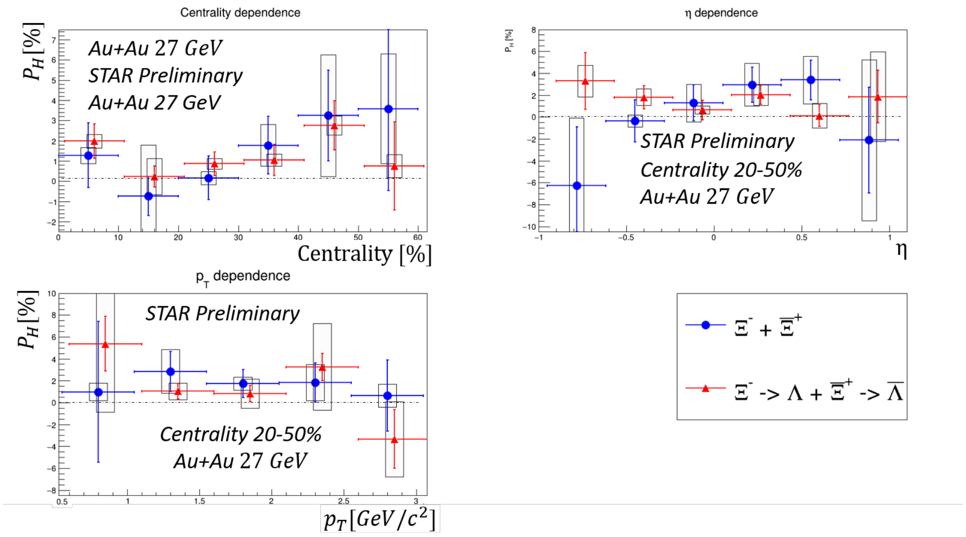

Fig. 3. Global polarization of Ξ hyperons in $\sqrt{s_{NN}} = 27$ GeV Au+Au collisions.

Figure 4 shows the global polarization as a function of collision energy. The Ξ polarization results are compared with Λ global polarization data from $\sqrt{s_{NN}} = 7.7$–200 GeV, BES-II Λ results at $\sqrt{s_{NN}} = 19.6$ and 27 GeV, and the prior Ξ polarization measurement at $\sqrt{s_{NN}} = 200$ GeV. The data are shown alongside theoretical predictions from the AMPT model [19]. The observed polarization for Ξ hyperons follows a trend similar to that of Λ hyperons and aligns with AMPT model calculations, supporting the hypothesis of a global nature of hyperon polarization in heavy-ion collisions.

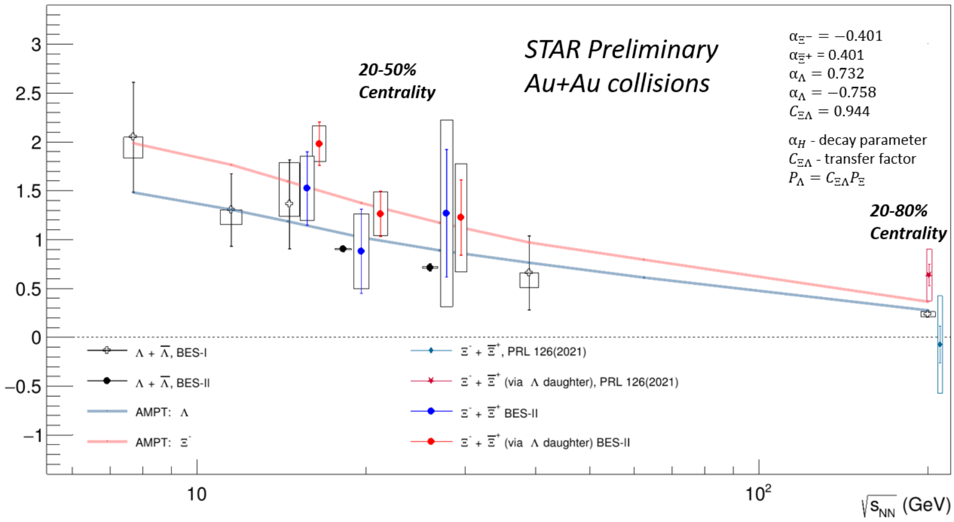

Fig. 4. Energy dependence of hyperon global polarization

Summary

We presented the results of global polarization measurements for $\Xi^- + \bar{\Xi}^+$ in Au+Au collisions at $\sqrt{s_{NN}}$ =14.6, 19.6 and 27 GeV measured directly via the angle of daughter Λ and via transfer to Λ daughter global polarization. These measurements of Ξ global polarization align with the global trends observed for hyperon global polarization and are consistent with theoretical predictions.

Acknowldedgements

The work was funded in part by the Ministry of Science and Higher Education of the Russian Federation, Project "New Phenomena in Particle Physics and the Early Universe" FSWU-2023-0073, and by the MEPhI Program Priority 2030. The work was partially performed using resources of NRNU MEPhI high-performance computing center.

REFERENCES

1. *Voloshin S.A., Poskanzer A.M., Snellings R.* Collective phenomena in non-central nuclear collisions. 2008. arXiv:0809.2949 [nucl-ex].

2. *Liang Z.T., Wang X.N.* Globally Polarized Quark-Gluon Plasma in Non-central $A+A$ Collisions // Phys. Rev. Lett. 2005. Mar. V. 94. P. 102301. URL: https://link.aps.org/doi/10.1103/PhysRevLett.94.102301.

3. *Voloshin S.A.* Polarized secondary particles in unpolarized high energy hadron-hadron collisions? 2004. arXiv:nucl-th/0410089.

4. *Voloshin S.A., Niida T.* Ultrarelativistic nuclear collisions: Direction of spectator flow // Phys. Rev. C. 2016. Aug. V. 94. P. 021901. URL: https://link.aps.org/doi/10.1103/PhysRevC.94.021901.

5. *Zyla P.A. et al.* [Particle Data Group Collaboration] Review of Particle Physics // Progress of Theoretical and Experimental Physics. 2020. 08. V. 2020, no. 8. 083C01 https://academic.oup.com/ptep/article-pdf/2020/8/083C01/34673722/ptaa104.pdf.

6. *Abelev B.I., Aggarwal M.M., Ahammed Z., Anderson B.D., Arkhipkin D., Averichev G.S., Bai Y., Balewski J., Barannikova O., Barnby L.S., et al.*. Global polarization measurement in Au+Au collisions // Physical Review C. 2007. Aug. V. 76, no. 2. URL: http://dx.doi.org/10.1103/PhysRevC.76.024915.

7. *Adamczyk L., et al.*. Global Lambda hyperon polarization in nuclear collisions // Nature. 2017. Aug. V. 548, no. 7665. P. 62–65. URL: http://dx.doi.org/10.1038/nature23004.

8. *Abdallah M.S. et al.* [STAR Collaboration] Global Λ-hyperon polarization in Au+Au collisions at $\sqrt{s_{\mathrm{NN}}} = 3$ GeV. 2021. 7. arXiv:2108.00044.

9. *Adam J. et al.* [STAR Collaboration Collaboration] Global Polarization of Ξ and Ω Hyperons in Au + Au Collisions at $\sqrt{s_{NN}} = 200$ GeV // Phys. Rev. Lett. 2021. Apr. V. 126. P. 162301. URL: https://link.aps.org/doi/10.1103/PhysRevLett.126.162301.

10. *Lee T.D., Yang C.N.* General Partial Wave Analysis of the Decay of a Hyperon of Spin $\frac{1}{2}$ // Phys. Rev. 1957. Dec. V. 108. P. 1645–1647. URL: https://link.aps.org/doi/10.1103/PhysRev.108.1645.

11. *Huang M. et al.* [HyperCP Collaboration] New Measurement of $\Xi^- \to \Lambda\pi^-$ Decay Parameters // Phys. Rev. Lett. 2004. Jun. V. 93. P. 011802. URL: https://link.aps.org/doi/10.1103/PhysRevLett.93.011802.

12. *Luk K.B., Diehl H.T., Duryea J., Guglielmo G., Heller K., Ho P.M., James C., Johns K., Longo M.J., Rameika R., et al.*. Search for DirectCPViolation in Nonleptonic Decays of Charged Ξ and Λ Hyperons // Physical Review Letters. 2000. Dec. V. 85, no. 23. P. 4860–4863. URL: http://dx.doi.org/10.1103/PhysRevLett.85.4860.

13. *Anerella M., et al.*. The RHIC magnet system // Nuclear Instruments and Methods in Physics Research Section A: Accelerators, Spectrometers, Detectors and Associated Equipment. 2003. V. 499, no. 2. P. 280 – 315. The Relativistic Heavy Ion Collider Project: RHIC and its Detectors URL: http://www.sciencedirect.com/science/article/pii/S016890020201940X.

14. *Adams J., Ewigleben A., Garrett S., He W., Huang T., Jacobs P., Ju X., Lisa M., Lomnitz M., Pak R., et al.*. The STAR event plane detector // Nuclear Instruments and Methods in Physics Research Section A: Accelerators, Spectrometers, Detectors and Associated Equipment. 2020. Jul. V. 968. P. 163970. URL: http://dx.doi.org/10.1016/j.nima.2020.163970.

15. *Whitten C.A. et al.* [STAR Collaboration] The beam-beam counter: A local polarimeter at STAR // AIP Conf. Proc. 2008. V. 980, no. 1. P. 390–396.

16. *Anderson M., Berkovitz J., Betts W., Bossingham R., Bieser F., Brown R., Burks M., Calderón de la Barca Sánchez M., Cebra D., Cherney M., et al.*. The STAR time projection chamber: a unique tool for studying high multiplicity events at RHIC // Nuclear Instruments and Methods in Physics Research Section A: Accelerators, Spectrometers, Detectors and Associated Equipment. 2003. Mar. V. 499, no. 2-3. P. 659–678. URL: http://dx.doi.org/10.1016/S0168-9002(02)01964-2.

17. *Llope W.* Multigap RPCs in the STAR experiment at RHIC // Nuclear Instruments and Methods in Physics Research Section A: Accelerators, Spectrometers, Detectors and Associated Equipment. 2012. V. 661. P. S110–S113. X. Workshop on Resistive Plate Chambers and Related Detectors (RPC 2010) URL: https://www.sciencedirect.com/science/article/pii/S0168900210017006.

18. *Maxim Z.* Online selection of short-lived particles on many-core computer architectures in the CBM experiment at FAIR // Ph.D. thesis, Johann Wolfgang Goethe-367 Universitat. 2016.

19. *Wei D.X., Deng W.T., Huang X.G.* Thermal vorticity and spin polarization in heavy-ion collisions // Phys. Rev. C. 2019. Jan. V. 99. P. 014905. URL: https://link.aps.org/doi/10.1103/PhysRevC.99.014905.